OPEN

Citation: Cell Death and Disease (2014) 5, e1130; doi:10.1038/cddis.2014.99
© 2014 Macmillan Publishers Limited All rights reserved 2041-4889/14
www.nature.com/cddis

# Homozygous mutation of MTPAP causes cellular radiosensitivity and persistent DNA double-strand breaks

NT Martin*[,1,2], K Nakamura[1], U Paila[3], J Woo[1], C Brown[1], JA Wright[4], SN Teraoka[4], S Haghayegh[1], D McCurdy[5], M Schneider[6], H Hu[1], AR Quinlan[3], RA Gatti[1,2,7] and P Concannon[4,8]

**The study of rare human syndromes characterized by radiosensitivity has been instrumental in identifying novel proteins and pathways involved in DNA damage responses to ionizing radiation. In the present study, a mutation in mitochondrial poly-A-polymerase (*MTPAP*), not previously recognized for its role in the DNA damage response, was identified by exome sequencing and subsequently associated with cellular radiosensitivity. Cell lines derived from two patients with the homozygous *MTPAP* missense mutation were radiosensitive, and this radiosensitivity could be abrogated by transfection of wild-type mtPAP cDNA into mtPAP-deficient cell lines. Further analysis of the cellular phenotype revealed delayed DNA repair, increased levels of DNA double-strand breaks, increased reactive oxygen species (ROS), and increased cell death after irradiation (IR). Pre-IR treatment of cells with the potent anti-oxidants, α-lipoic acid and n-acetylcysteine, was sufficient to abrogate the DNA repair and clonogenic survival defects. Our results firmly establish that mutation of the *MTPAP* gene results in a cellular phenotype of increased DNA damage, reduced repair kinetics, increased cell death by apoptosis, and reduced clonogenic survival after exposure to ionizing radiation, suggesting a pathogenesis that involves the disruption of ROS homeostasis.**
*Cell Death and Disease* (2014) **5,** e1130; doi:10.1038/cddis.2014.99; published online 20 March 2014
**Subject Category:** Cancer

XCIND syndrome (X-ray sensitivity, Cancer predisposition, Immunodeficiency, Neurologic involvement, and DNA double-strand break repair deficiency) is a pleiotropic syndrome of radiosensitivity disorders resulting from mutation of DNA damage recognition and repair genes.[1,2] Ataxia-telangiectasia (A-T) is the archetypal XCIND syndrome disorder and results from mutation of the ataxia-telangiectasia-mutated (*ATM*) protein kinase gene.[3] A-T patients manifest both cellular and clinical hypersensitivity to ionizing radiation, which results from disruption of the nuclear function of ATM in the recognition and response to DNA double-strand breaks (DSBs).[4,5] Additional radiosensitivity disorders have been identified since A-T was first characterized, and, to date, have involved mutations in DNA DSB recognition or repair genes.[2,6]

Recognition and repair of DSBs is a complex and dynamic process involving at least two main repair pathways, non-homologous end joining (NHEJ) and homologous recombination (HR) repair. The MRN complex (meiotic recombination 11 homolog (*S. cerevisiae*), Rad50, and Nijmegen breakage syndrome 1 (NBS1)) and ATM are initial sensors of DSBs and are recruited to nuclear foci surrounding breaks.[7] Loss of a single member of the MRN complex results in cellular radiosensitivity and clinical features that overlap with A-T.[8–11] Recognition of DSBs by the MRN complex and ATM initiates a signaling cascade leading to the activation of cell cycle checkpoints and the recruitment of other repair proteins, such as H2A histone family, member X, phosphorylated serine 139 (γ-H2AX) and p53-binding protein 1 (53BP1), to the sites of DSBs.[12–15]

γ-H2AX forms nuclear foci that persist throughout the repair process and disengage once the repair process has been completed.[16] The initial recruitment of MRN, ATM, and γ-H2AX is followed by recruitment of the 53BP1 repair protein via a chromatin ubiquitin ligase cascade.[17–19] 53BP1

[1]UCLA Department of Pathology and Laboratory Medicine, MacDonald Research Laboratories, Los Angeles, CA, USA; [2]UCLA Biomedical Physics Interdepartmental Graduate Program, Los Angeles, CA, USA; [3]Department of Public Health Sciences, Center for Public Health Genomics, University of Virginia, Charlottesville, VA, USA; [4]Genetics Institute, University of Florida, Gainesville, FL, USA; [5]UCLA Department of Pediatrics, Los Angeles, CA, USA; [6]Carle Physician Group, Urbana, IL, USA; [7]UCLA Department of Human Genetics, Los Angeles, CA, USA and [8]Department of Pathology, Immunology and Laboratory Medicine, University of Florida, Gainesville, FL, USA

*Corresponding author: NT Martin, UCLA Department of Pathology and Laboratory Medicine, MacDonald Research Laboratories, 675 Charles E Young Dr. South, Room 4-609, Los Angeles, CA 90095-1732, USA. Tel: +1 310 825 7200; Fax: +1 310 825 7618; E-mail: namartin@mednet.ucla.edu
**Keywords:** radiosensitivity; MTPAP; DNA repair; sequencing; reactive oxygen species; DNA damage
**Abbreviations:** 53BP1, p53-binding protein 1; A-T, ataxia-telangiectasia; α-LA, α-lipoic acid; ATM, ataxia-telangiectasia mutated; BRCA1, breast cancer 1, early onset; CSA, clonogenic survival assay; DCHF-DA, dichloro-dihydro-fluorescein diacetate; DDR, DNA damage response; DHE, dihydroethidium; DSB, DNA double-strand break; FCCP, protonophore carbonyl cyanide p-(trifluoromethoxy)phenylhydrazone; γ-H2AX, H2A histone family, member X, phosphorylated serine 139; Gy, Gray; HR, homologous recombination; IR, irradiation (ionizing); INDEL, insertion-deletion; LCL, lymphoblastoid cell line; MRN, protein complex; MRE11, NBS1, RAD50; MTPAP/mtPAP, mitochondrial poly-A-polymerase; NAC, n-acetyl cysteine; NBS1, Nijmegen breakage syndrome 1; NCA, neutral comet assay; NHEJ, non-homologous end joining; Oligo, oligomycin; RAD50, RAD50 homolog (*S. cerevisiae*); RAD51, RAD51 recombinase; ROS, reactive oxygen species; SF%, survival fraction percentage; SMC1, structural maintenance of chromosomes 1; TM, tail moment; WT, wild type; XCIND, X-ray sensitivity, cancer predisposition, immunodeficiency, neurologic involvement, DNA repair defect
Received 17.12.13; revised 29.1.14; accepted 03.2.14; Edited by A Finazzi-Agró

is important for modulating the choice of repair pathway between NHEJ, the dominant DSB repair mechanism, and HR, an error-free repair mechanism active in late S and G2 phase cells because it requires homologous chromatids.[20,21] When 53BP1 is displaced from the sites of DSBs by the breast cancer susceptibility protein, BRCA1 (breast cancer 1, early onset), end resection via CtBP-interacting protein (CtIP) and the MRN complex occurs to initiate homologous recombination repair.[21–23] Recently, reduction of CtIP levels was shown to disrupt BRCA1 focus accumulation leading to DSB repair defects and cellular radiosensitivity.[24] The DNA repair protein RAD51 recombinase (RAD51) is also recruited to the sites of DSBs after BRCA1 localization when HR repair is occurring.[25,26]

Although much of what is known about the cellular response to ionizing radiation is focused on molecules that accumulate at the sites of damage, the cellular environment would also be expected to have an important supporting role in facilitating these responses and maintaining genomic stability. Ionizing radiation generates DSBs via direct interaction with DNA. Many more breaks are generated from reactive oxygen species (ROS) that also cause oxidative and mitochondrial stress.[27,28] Cellular ROS homeostasis and ATP levels are required for supporting DNA repair, and protecting against DSBs generation, and mitochondria are the main mediators of these levels.[29–32] In addition, mitochondria act as central modulators of apoptotic cell death, which has an important role in removing cells with persistent or oncogenic DNA lesions.[27,33] Thus, mitochondria would be expected to have a central role in the DNA damage response (DDR). Several studies focusing on mutations in mitochondrial genes have indicated dysfunction of mitochondrial ATP production, dysregulation of DSB repair gene expression, and genomic instability.[30,34–36] However, the exact mechanism by which mitochondrial dysfunction, such as that induced by mutation of genes important for mitochondrial function, can reduce survival after radiation exposure remains unclear.[34–36]

In the present study, exome sequencing identified a homozygous 1432A>G DNA variant encoding the missense change N478D in the mitochondrial poly-A-polymerase (*MTPAP*) gene in two siblings of an Amish family affected with spastic ataxia. Lymphoblastoid cell lines (LCLs) derived from these siblings were radiosensitive, based on colony survival fraction post-irradiation (IR). Although the homozygous 1432A>G *MTPAP* variant was previously associated with spastic ataxia in an Amish pedigree, the listed features of the affected individuals did not include radiosensitivity. Therefore, the association of homozygous 1432A>G with sensitivity to ionizing radiation was tested by transfecting the patient-derived LCLs with wild-type (WT) *MTPAP* and assaying clonogenic survival. The *MTPAP* variant LCLs were also assessed for levels of DNA damage and repair, ROS, mitochondrial respiration, and apoptosis in order to elucidate pathways by which mtPAP influences cellular responses to ionizing radiation.

## Results

**Radiosensitivity segregated with bi-allelic mtPAP mutations in RS63 family.** Two affected siblings from a consanguineous Amish family were tested for reduced colony survival levels post-IR, a radiosensitive phenotype, because they displayed a clinical phenotype similar to A-T. Both affected siblings, RS63-3 and RS63-7, were characterized by ataxia with initiation tremors. Growth failure, developmental delay, and spasticity were also noted, whereas no immune deficiencies or tumors have been observed to date. There was AT-like reduced colony survival in RS63-3 and -7.[4] Unaffected siblings (RS63-4, -5, -6) had normal colony survival post-IR (Figure 1a). The neutral comet assay (NCA) is another useful method for assessing DNA DSB repair fidelity and correlates well with the clonogenic survival assay (CSA).[37] RS63-3 and -7 demonstrated an AT-like DSB repair defect, consistent with the CSA result, and the unaffected siblings of the family were found to have normal levels of DNA repair (Figure 1b).[37]

The AT-like cellular and clinical phenotype strongly suggested a diagnosis of A-T, however, ATM protein expression was normal. Exome sequencing was employed

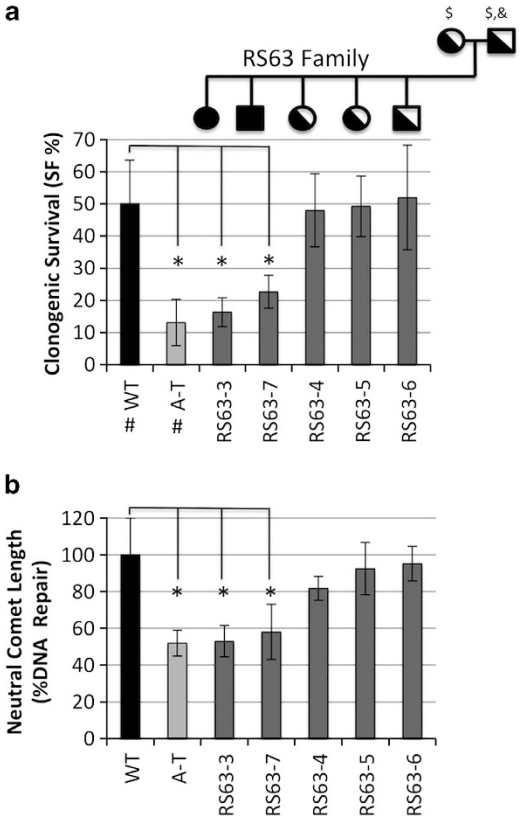


**Figure 1** Cellular radiosensitivity and DNA repair defect segregated with affected members of RS63 family with a homozygous mutation of mtPAP. (**a**) The survival fraction (SF%) measured by the CSA (at 1 Gy) is reduced in the two members of the RS63 family, RS63-3 and -7, who are homozygous for the *MTPAP* mutation. The '#' indicates SF% representative of WT and highly radiosensitive (A-T) cells used for comparison in clinical radiosensitivity testing based on Sun *et al*.[4] The '$' denotes patients for whom we were not able to generate an LCL. The '&' denotes that we were unable to obtain DNAs for *MTPAP* sequencing analysis; however, the father is an obligate heterozygote. (**b**) The neutral comet assay, measuring predominately DNA DSBs, reveals an AT-like DNA repair defect in RS63-3 and -7. Results are displayed as percent DNA repair (% repair) post-15 Gy and represent the return of comet tails to baseline levels at 5 h post-IR. An asterisk denotes statistical significance at $P<0.05$

as an untargeted approach to identify candidate causative mutations in other genes. At the time of initial sequencing, only an LCL derived from RS63-3 was available. Comparison of the RS63-3 exome sequence to the human reference sequence confirmed the absence of ATM mutations, but identified 36 563 coding variants relative to the reference, 690 of which were unique to RS63-3. Based upon the consanguinity in the RS63 family, the variants were filtered for homozygosity, yielding 26 coding variants. Variants predicted to be deleterious because they would result in gain or loss of a stop codon, a frameshift or a non-synonymous substitution at a conserved amino-acid position, and were not observed in either the NHLBI Exome Sequencing Project or the 1000 Genomes Project were identified. This yielded *hornerin* and *MTPAP* as candidate variants. These two genes were manually examined to determine which might have a role in the DDR or in cerebellar development or function. The homozygous missense mutation (c.1432A>G, N478D) in the *MTPAP* gene was singled out because it had been previously associated with spastic ataxia and optic atrophy and was the only one of the two possible variants predicted to be deleterious by Polyphen.[38,39] The 1432A>G *MTPAP* mutation, and lack of ATM mutations, was later confirmed in RS63-7 once a cell line could be derived. The unaffected siblings (RS63-4, -5, -6) and mother were heterozygous for the *MTPAP* mutation, suggesting autosomal recessive inheritance (Supplementary Figure 1).

**Mutation of mtPAP was causally linked to the radiosensitive and persistent DNA damage phenotype by mtPAP transfection.** *MTPAP* is nuclear encoded, poly-adenylates mitochondrial transcripts, and, unlike nuclear polyadenylation polymerases, has a variable affect on transcript stability.[38,40,41] Thus, it was unclear how mutation of *MTPAP* might result in radiosensitivity. The AT-like radiosensitivity (Figure 2a) and DNA repair defect (Figure 2b and Supplementary Figure 2) observed in RS63-3 and -7 were rescued when WT mtPAP cDNA was transfected into the patient's LCLs, confirming a causal link between *MTPAP*, cellular radiosensitivity, and defective DNA repair.

**Increased post-IR DNA DSB induction in RS63-3 and -7.** The similarities in clinical phenotype between RS63-3 and RS63-7 and A-T patients led us to consider that mutation of *MTPAP* might impact the ATM signaling cascade. We screened a panel of ATM kinase activity biomarkers, including ATM autophosphorylation and downstream phosphorylation of structural maintenance of chromosomes 1 (SMC1), KRAB-associated protein 1 (KAP1), and NBS1, which are necessary for detection of DSBs and transmission of the DDR signal.[7,13,14,42] Phosphorylation of ATM, SMC1, KAP1, and NBS1 in cell lysates from RS63-3 and -7 was WT-like post-IR, indicating that mtPAP does not likely impact early ATM kinase signaling (data not shown). We have shown that monitoring $\gamma$-H2AX, 53BP1, and BRCA1 foci kinetics post-IR can be used to characterize DDR defects in radiosensitive patients of unknown etiology by comparing kinetic curves to those of known radiosensitivity disorders.[43] RS63-3 and -7

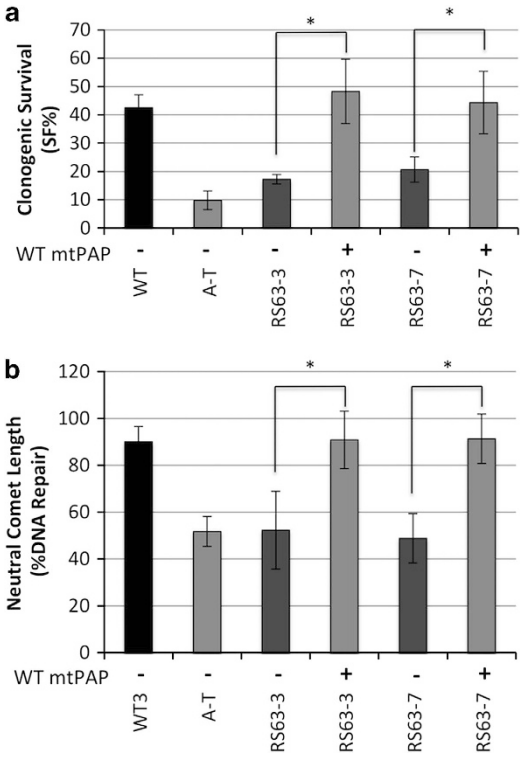


**Figure 2** Transfection of WT mtPAP into RS63-3 and -7 rescued radiosensitivity and DNA repair defects. (**a**) Transfection of WT mtPAP cDNA (+) into RS63-3 and -7 rescued the radiosensitive (i.e., reduced SF%) phenotype measured by the CSA (at 1 Gy). A (+) denotes transfection with WT mtPAP cDNA and (−) denotes transfection with an empty vector. (**b**) WT mtPAP (+) or control plasmid (−) was transfected into RS63-3 and -7; the WT mtPAP plasmid rescued the DNA DSB repair defect as measured by the NCA (at 15 Gy). '% DNA repair' represents the return to baseline tail moment (TM) measure of DNA damage 5 h post-IR and is the $TM_{no\ IR}/TM_{5h}$. An asterisk denotes statistical significance at $P<0.05$

displayed normal basal levels of $\gamma$-H2AX foci and normal repair kinetics at 4, 8, and 24 h; however, the 1 h post-IR response was increased in both LCLs, suggesting increased levels of DSB induction (Figure 3a). Similarly, increased DSB levels post-IR in RS63-3 and -7 were noted by the NCA (Figure 3b). Increased levels of 53BP1 foci were also observed 1 h post-IR and persisted at 4 h (Supplementary Figure 3A). Finally, BRCA1 and RAD51 foci were assessed as markers of HR.[26,44] A trend toward reduced BRCA1 foci-positive cells, compared with WT, at 4 h was observed followed by a significant reduction in foci numbers at 8 h post-IR, suggesting either a defect in recruitment of BRCA1 to DSBs or a shift away from initiating HR (Supplementary Figure 3B). Consistent with reduced HR repair, RAD51 foci were also reduced at 8 h post-IR (Supplementary Figure 3C).

HR is only active in the late S and G2 phases of the cell cycle and, thus, we hypothesized that cell cycle perturbations might impact the reductions observed in BRCA1 and RAD51 foci numbers at 8 h. Cell cycle distribution was assessed in RS63-3 and -7 and was found to be WT-like before and after IR (Supplementary Figure 4). Similarly, the fidelity of the S-phase and G2/M phase checkpoints were WT-like (Supplementary Figures 5 and 6). Thus, our data suggest that the reductions in BRCA1 and RAD51 foci were not due to

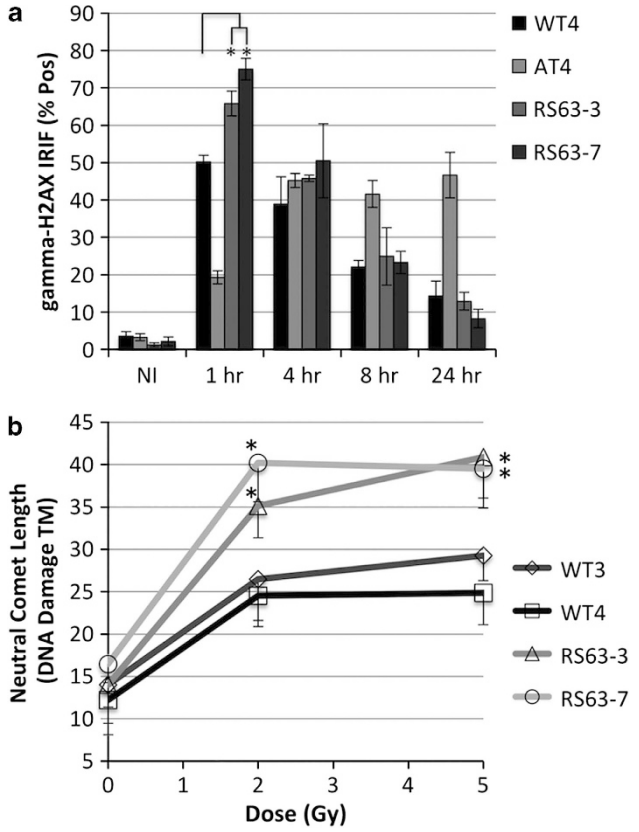


**Figure 3** Increased induction of DNA damage post-IR in RS63-3 and -7. (**a**) $\gamma$-H2AX irradiation-induced foci (IRIF) were increased at 1 h (post-2 Gy) in RS63-3 and -7 compared with WT levels. The results are expressed as the percentage of cells positive for four or more foci/nuclei (% Pos). WT4 is a representative WT response. Asterisks denote statistical significance at $P<0.05$. (**b**) DNA DSB levels were assessed immediately post-2 and -5 Gy. Increased levels of DSBs were observed in RS63-3 and -7. Asterisks indicate statistical significance at the $P<0.05$ level comparing RS63-3 and -7 ($n=4$, each) to both WT3 and WT4 ($n=4$, each)

large differences in cell cycle distribution, nor checkpoint activation, and that cell cycle control was not significantly impacted by mutation of *MTPAP*.

**Normal mitochondrial respiration, increased ROS levels, and increased apoptosis in RS63-3 and -7 post-IR.** Mitochondria are closely involved in the DDR by at least three mechanisms: (1) maintaining ROS homeostasis, (2) mediating apoptotic signals, and (3) producing energy needed for DSB repair.[27,30] Owing to the known function of mtPAP in the mitochondria, we postulated that mutation of *MTPAP* might result in dysfunctional mitochondria and subsequent disruption of the DDR. Mitochondrial respiration levels were assessed with the rezasurin dye. Contrary to our working model, basal mitochondrial respiration was normal in RS63-3 and -7 (Figure 4a). Mitochondrial bioenergetics were further probed by measuring the oxygen consumption rate after addition of oligomycin (Oligo; ATP synthase inhibitor), FCCP (protonophore carbonyl cyanide p-(trifluoromethoxy)-phenylhydrazone; respiratory chain uncoupler), and rotenone/myxothiazol (R/M; mitochondrial respiration inhibitors). Basal respiration (time 1–3), ATP-linked respiration (time 4–6), and total mitochondrial respiration levels (time 10–14) were largely similar to WT levels in RS63-3 and -7. However, maximal mitochondrial respiration levels (time 7–9), induced by addition of FCCP, were greatly increased in RS63-3 and -7 (Figure 4b). Transfection of WT mtPAP cDNA into RS63-3 and -7 partially abrogated the increased maximal respiration after addition of FCCP phenotype (time 7-9), and returned respiration levels closer to WT levels (Supplementary Figure 7).

Abnormal ROS levels have been linked to reduced colony survival and DSB repair, and mitochondria are known to be the main producers, and reducers, of many ROS.[27,45] Dichloro-dihydro-fluorescein diacetate (DCHF-DA), a dye that can react to a broad array of ROS moieties, was used to assess ROS levels in RS63-3 and -7. Increased ROS levels were observed in RS63-3 and -7 post-IR, similar to those of A-T LCLs (Figure 4c and Supplementary Figure 8A).[46] These data would suggest that the antioxidant responses in RS63-3 and -7 were not functioning optimally, post-IR. However, given the increased maximal respiration in RS63-3 and -7, we postulated that some of the ROS may be entering the cytosol through leaky or dysfunctional mitochondria. Superoxide is the main ROS moiety that could leak from dysfunctional respiration and dihydroethidium (DHE) dye, a cell permeable dye preferentially detecting superoxide radicals, was used to assess superoxide levels.[47] Increased basal superoxide levels were observed in RS63-3 and -7, further supporting the notion of mitochondrial dysfunction (Supplementary Figure 8B). Superoxide levels were not significantly induced in WT-LCLs post-10 Gy, but there were significant increases in superoxide levels post-IR in RS63-3 and -7 (Supplementary Figure 8B). Transfection of WT mtPAP cDNA into RS63-3 and -7 partially abrogated the increased basal superoxide levels observed in RS63-3 and -7, and rescued the IR-induced increase in superoxide levels (Supplementary Figure 8C). Owing to technical limitations (i.e., fluorescent spectra overlap between the GFP tag for the cDNA constructs and DCHF-DA), we were unable to also demonstrate rescue of the IR-induced ROS levels with this more general dye for ROS in RS63-3 and -7. Consistent with cells undergoing oxidative stress, increased apoptosis levels were found in RS63-3 and -7 post-IR (Figure 4d).[27]

**Antioxidants, $\alpha$-lipoic acid ($\alpha$-LA) and n-acetylcyseine, rescued mtPAP-deficient cellular radiosensitivity and DNA repair phenotype.** The increased levels of ROS were intriguing, but it was unclear whether this contributed to the cellular phenotype of RS63-3 and -7. To test this, $\alpha$-LA, a potent antioxidant, was used to lower ROS levels.[48] $\gamma$-H2AX foci levels were assessed at 1-h post-IR to determine whether increased levels of foci in RS63-3 and -7 could be returned to WT levels by $\alpha$-LA. Indeed, pre-treatment with $\alpha$-LA at concentrations $>1\,\mu$M reduced $\gamma$-H2AX foci levels to WT levels (Figure 5a). Interestingly, $\alpha$-LA treatment had no effect on $\gamma$-H2AX foci levels in WT-LCLs at the concentrations tested. When assessed by the NCA, the increased levels of DSBs initially induced post-IR in RS63-3 and -7 were also abrogated by pre-IR treatment with $\alpha$-LA, confirming protection against elevated IR-induced damage (Supplementary Figure 9). The DNA repair defect measured

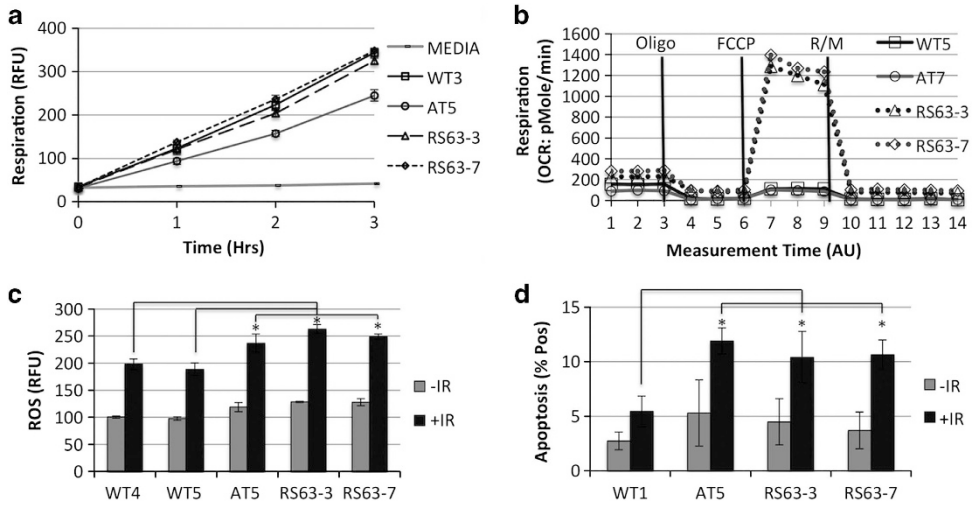


**Figure 4** RS63-3 and -7 LCLs had normal mitochondrial respiration but increased levels of ROS and apoptosis post-IR. (**a**) Mitochondrial respiration was measured by monitoring metabolism of the rezasurin dye and indicated WT-like, or normal, respiration in RS63-3 and -7. The results are displayed as relative fluorescent units (RFUs) of the metabolized rezasurin dye. WT3 is a representative WT-LCL response. AT5 is a representative A-T cell with a characteristic mitochondrial defect.[37] (**b**) Mitochondrial bioenergetics were profiled using the XF24 Extracellular Flux Analyzer, and RS63-3 and -7 had increased maximal respiration levels after addition of FCCP, compared with WT-LCLs. WT5 is a representative WT-LCL response. The oxygen consumption ratio (OCR) was measured as an indicator of mitochondrial respiration. (**c**) Reactive oxygen species (ROS) levels were assessed using DCHF-DA dye (RFU). Increased IR-induced levels of ROS were noted in RS63-3 and -7. Asterisks denote statistical significance at the $P<0.05$ level comparing the $+$ IR condition of the indicated sample to both of the WT4 and WT5 $+$ IR conditions. (**d**) Apoptosis was determined by FACS analysis of cells positive for Annexin V staining 48 h post-10 Gy, and indicates increased post-IR apoptosis in RS63-3 and -7. Asterisks indicate statistical significance at the $P<0.05$ level

by the NCA was also rescued in RS63-3 and -7 by pre-IR treatment with 1 $\mu$M $\alpha$-LA (Figure 5b). Further, pre-IR $\alpha$-LA treatment rescued the radiosensitive phenotype, but had no affect on WT or A-T LCLs (Figure 5c). The lack of survival fraction percentage (SF%) improvement with $\alpha$-LA treatment in A-T LCLs is consistent with previous findings and further elucidates the differential dependency of radiosensitivity and ROS levels in WT, A-T, and mtPAP-deficient LCLs.[49]

Recently, however, $\alpha$-LA has been shown to modulate ATP synthase levels and mitochondrial DNA content, which might also modulate DDRs.[50] To rule out phenomena specific to a single antioxidant, $\alpha$-LA, we tested whether n-acetylcisteine (NAC), another potent antioxidant, could also abrogate the radiosensitive cellular phenotype in RS63-3 and -7. Pre-treatment of cells with NAC protected against increased DNA DSB induction (Supplementary Figure 10A), rescued the delay in DNA repair (Supplementary Figure 10B), and restored clonogenic survival to WT levels in RS63-3 and -7 (Supplementary Figure 10C).

## Discussion

We describe two Amish siblings (RS63-3 and -7) with a homozygous *MTPAP* mutation that had been previously associated with spastic ataxia in an Old Order Amish population and can now be causally linked to radiosensitivity and modulation of the DDR.[38] Identification of *MTPAP* as a candidate gene responsible for the defects observed in these patients was initially enabled by exome sequencing of DNA from these patients. However, as is common with exome sequencing, many variants were identified that were potentially disease causing. With the expectation of homozygosity in the disease-causing variant, the variant list was narrowed and led to selection of the N478D missense mutation in mtPAP as a candidate radiosensitivity gene because it was previously shown to segregate with spastic ataxia in the Old World Amish population; a similar phenotype to RS63-3 and -7.[38] This would be the first radiosensitivity associated gene identified by exome-sequencing approaches in patients. Colony survival testing indicated that LCLs derived from RS63-3 and -7 were radiosensitive, a new clinical phenotype for spastic ataxia associated with *MTPAP* mutation. The NCA further indicated a DNA repair defect in RS63-3 and -7. Crucially, transfection of WT *MTPAP* into RS63-3 and -7 cells abrogated both the DSB repair defect and the reduction in clonogenic survival, confirming that mutation of *MTPAP* is responsible for the cellular radiosensitivity phenotype.

mtPAP is a nuclear-encoded mitochondrial polyadenylation polymerase that was not an obvious candidate for causing radiosensitivity.[38,41] Examination of ATM expression and kinase activity indicated that it was unlikely that mutation of mtPAP disrupts ATM-mediated signaling or is required for the early recognition of DSBs. Increased $\gamma$-H2AX and 53BP1 foci at 1 h, and persistent 53BP1 foci at 4 h were observed, suggesting disruption of the DDR early post-IR, but independent of the initial sensing of DSB damage by ATM. Increased induction of DNA damage post-IR relative to WT levels was suspected in RS63-3 and -7, and was confirmed by increased comet tails measured by the NCA. These results suggest that mutation of mtPAP may affect the induction of DSBs rather than their recognition or repair, a potential deviation from the classical presentation of human radiosensitivity disorders.

Interestingly, general ROS levels and superoxide radical levels were also increased in RS63-3 and -7. It has been known that mitochondrial function is important for maintaining ROS homeostasis before and after exogenous insults and

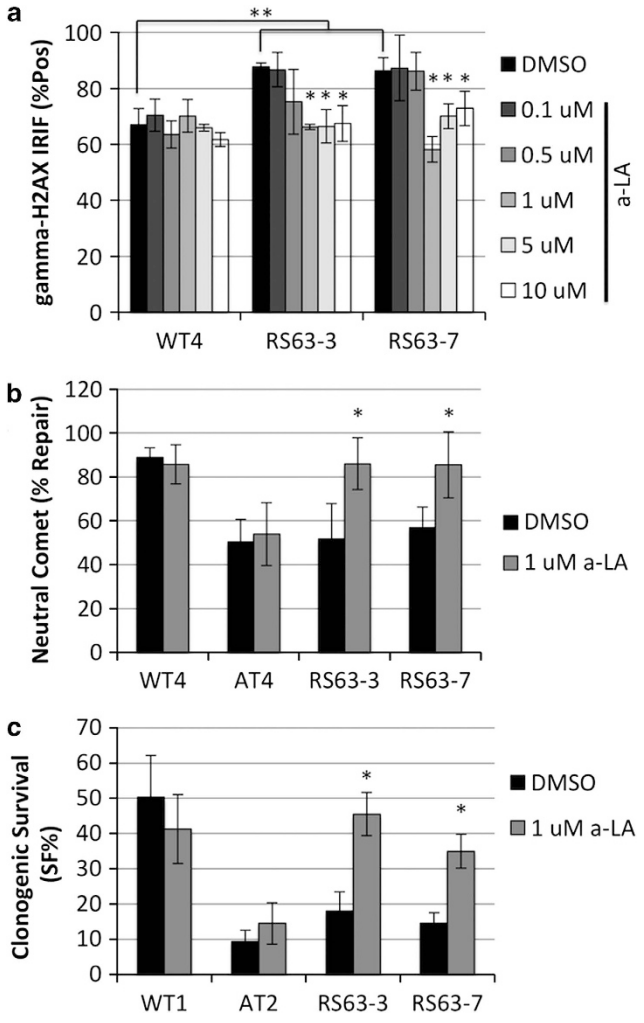


**Figure 5** Anti-oxidant $\alpha$-lipoic acid ($\alpha$-LA) reduced initial $\gamma$-H2AX foci levels, rescued repair defect, and abrogated radiosensitivity in RS63-3 and -7. (**a**) $\gamma$-H2AX foci were assessed 1-h post-2 Gy after overnight treatment with $\alpha$-LA or vehicle control (DMSO). Pre-IR treatment with $\alpha$-LA $>1$ $\mu$M abrogated the increased $\gamma$-H2AX foci phenotype in RS63-3 and -7, restoring WT-like levels of $\gamma$-H2AX foci-positive cells. One asterisk indicates statistical significance at the $P<0.05$ level comparing $\alpha$-LA-treated samples to vehicle control samples for each cell line. Two asterisks indicate significance at the $P<0.05$ level comparing vehicle control samples across cell lines. (**b**) Pre-IR treatment of RS63-3 and -7 with 1 $\mu$M $\alpha$-LA abrogated the post-IR DNA repair defect measured by the NCA. Comets resulting from unrepaired DSBs were assessed post-15 Gy and results are presented as '% Repair', which is the return to baseline levels of damage 5-h post-IR ($TM_{no\ IR}/TM_{5h}$). Asterisks indicate statistical significance at the $P<0.05$ level when comparing $\alpha$-LA-treated samples to vehicle control samples. (**c**) Cellular radiosensitivity, indicated by reduced SF% post-1 Gy, was rescued in RS63-3 and -7 by pre-treatment with 1 $\mu$M $\alpha$-LA. Asterisks denote statistical significance at the $P<0.05$ level when comparing $\alpha$-LA-treated samples to vehicle control samples

that, when dysfunctional, mitochondria can leak superoxide radicals into the cytosol and can impair antioxidant response mechanisms.[29] These ROS levels can impact the number and complexity of DSBs through the induction of single or many clustered single-strand breaks.[31] The increased level of 53BP1 foci and decrease in both BRCA1 and RAD51 foci post-IR may indicate a shift away from HR repair, which may fail with clustered complex breaks, and a preference toward NHEJ repair.

Based on the known function of mtPAP, we postulated that the increased ROS levels were due to dysregulation of mitochondria function. Contrary to our prediction, basal respiration levels were WT-like in RS63-3 and -7. However, using the cellular bioenergetics assay, we found that there was a significant difference in maximal respiration levels in RS63-3 and -7 compared with WT levels when the respiratory chain decoupling agent, FCCP, was added to cells. The mitochondrial respiratory chain produces ROS moieties and, when deregulated, can leak ROS, especially superoxide radicals, into the cellular compartment producing a state of oxidative stress.[51] Transfection of WT mtPAP cDNA into RS63-3 and -7 partially reduced maximal mitochondrial respiration, basal superoxide levels, and IR-induced increases in superoxide levels to WT-like levels. These findings suggested that mutation of *MTPAP* is, indeed, disrupting mitochondrial function and resulting in increased levels of ROS before and after IR. Because of technical limitations, we were unable to demonstrate a causal link between generally increased post-IR ROS levels measured by DCHF-DA, a dye sensitive to multiple ROS moieties, and mutation of *MTPAP*. Ionizing radiation predominately induces different ROS moieties than superoxide, namely the hydroxyl radical, and it is likely that post-IR increases in ROS levels measured by the DCHF-DA dye reflect ROS moieties other than superoxide released from dysfunctional mitochondria. The increased levels of ROS measured by DCHF-DA, while reflecting the increase in superoxide levels in RS63-3 and -7, also may reflect reduced antioxidant response pathways to IR-induced hydroxyl radicals or other ROS that stem from other pathways, such as ROS induced by DNA damage.[52] Nevertheless, the data presented in this study supports a working model whereby mutation of *MTPAP* results in mitochondrial dysfunction and unbalanced ROS homeostasis through increased levels of pre-IR and post-IR ROS.

We explored the importance of ROS for modulating the RS63-3 and -7 cellular phenotype by pre-treating LCLs with the antioxidants, $\alpha$-LA and NAC. Pre-treatment with $\alpha$-LA and NAC abrogated the increased DNA damage levels, reduction in repair, and radiosensitivity in RS63-3 and -7. These results are consistent with our hypothesis that increased ROS levels negatively impact upon the response to ionizing radiation in cells with *MTPAP* mutations. The possibility of treating patients with *MTPAP* mutations with $\alpha$-LA and NAC is clinically intriguing as well. Both NAC and $\alpha$-LA are FDA-approved antioxidants that come in many formulations and represent attractive potential therapeutic approaches for patients harboring mutations in the *MTPAP* gene to protect against DSBs and chromosomal instability induced by oxidative stress.[31,45] In the studies reported herein, pre-treatment of WT and A-T LCLs with $\alpha$-LA had no affect on DNA repair nor clonogenic survival, whereas previous studies have indicated that antioxidants can improve other aspects of the A-T cellular phenotype.[46,49] Similar to $\alpha$-LA, NAC has been shown to modulate DNA damage levels at higher concentrations than those used in this study, but that NAC does not improve clonogenic survival.[49] The contrasting response to $\alpha$-LA between A-T and mtPAP-deficient patient cells underscores the differential causes of the radiosensitive phenotype in these patients.[46,49]

The A-T LCLs illustrate a classic model of radiosensitivity and XCIND, whereby increased levels of ROS are secondary to a core DSB recognition and repair defect arising from mutation of a core DDR gene. Thus, modulating ROS levels has little impact on DSB repair or clonogenic survival.[46] Conversely, the data for RS63-3 and -7 indicate that ROS levels increased DSB induction, resulted in reduced repair, and led to reduced clonogenic survival in these cells. The data suggest a potentially atypical mechanism of radiosensitivity and XCIND, where there is not mutation of a core DDR gene but, rather, a mutation in a gene leading to amplified induction of DNA damage by ionizing radiation. This might also account for the absence of immunodeficiency and cancer in mtPAP-deficient patients that would be expected if these patients followed a more classical AT-like presentation of the XCIND syndrome.

## Materials and Methods

**Cell culture, IR, and antioxidant treatment.** LCLs were derived from lymphocytes isolated from whole blood submitted for radiosensitivity testing as previously described.[4] LCLs were cultured in RPMI1640 media with 10% FBS, 1% streptomycin/penicillin/glutamine (Invitrogen, Carlsbad, CA, USA) and maintained at 37 °C in 5% $CO_2$. Cells were harvested for experiments when growing under log growth phase conditions and IR was carried out using a Mark IV Cs-137 sealed-source irradiator at a dose rate of $\sim$4.5 Gy/min. Where indicated, LCLs were treated overnight with $\alpha$-LA in DMSO or NAC in $H_2O$ (Sigma-Aldrich, St. Louis, MO, USA) before IR.

**WT mtPAP plasmid and transfection.** The open reading frame of human mtPAP (1749 bp) was PCR amplified from WT-LCLs using the following primers: Xba-mtPAP forward (5′-gacTCTAGAATGGCGGTTCCCGGCGTGGGGC TCT-3′) and Mlu-mtPAP reverse (5′-gacACGCGTTCATGTCTGAGTACTAATTGT TCTC-3′) and subcloned into a TA-vector using the manufacture's protocol (Invitrogen) to generate the WT mtPAP plasmid. The resulting product was sequenced to confirm WT mtPAP cDNA sequence. The TA-cloned mtPAP cDNA was then digested with *Xba*I and *Mlu*I restriction enzymes and the purified fragment was ligated into *Xba*I-*Mlu*I-digested (New England Biolabs, Ipswich, MA, USA), SAP-treated (Clontech, Mountain View, CA, USA), lenti 308 plasmid vector containing GFP (UCLA Vector Core, Los Angeles, CA, USA). Once the plasmid was generated, $\sim 15 \times 10^6$ LCLs were transiently transfected with 15 $\mu$g of Lenti-mtPAP/GFP (WT mtPAP) or Lenti-GFP control (CTL) expression constructs using electroporation (250 V, 1180 $\mu$F) in a Cell-Porator (Invitrogen). Cells were harvested for experiments two days after transfection. Transfection efficiencies were estimated at $\sim$80% by fluorescent microscopy imaging of GFP-positive cells.

**CSA.** The CSA for cellular radiosensitivity testing was performed on LCL samples as previously described.[4] Briefly, LCLs were seeded in a 96-well plate. The plates were treated with 1 Gy or sham-IR and returned to the incubator for 10–14 days. Wells positive for at least a single colony of $>$32 cells (i.e., five generations) were scored as positive and results were compared with sham-treated plates to determine the SF%.[4]

**Neutral comet assay.** The NCA for assessing DNA repair capacity of LCLs has been previously optimized by Nahas *et al.*[37] The Comet Assay kit (Trevigen Inc, Gaithersburg, MD, USA) was used under neutral conditions according to the manufacturer's specifications. LCLs were treated with 15 Gy or sham treated and collected at 0 h (no-IR), 30 min, and 5-h post-IR. LCLs were re-suspended in 1% low-melting-point agarose (Sigma-Aldrich) and plated on 20-well comet assay slides. Once the agarose solidified, the slides were added to a bath of cell lysis solution (Trevigen Inc) overnight at 4 °C. The following day, the samples (i.e., the free DNA fragments) on the slides were electrophoresed and stained using SYBR Gold (Invitrogen). Comets were visualized using an Olympus fluorescent microscope (Olympus, Tokyo, Japan) equipped with an AxioVision camera and software (Zeiss, Oberkochen, Germany). The tail moments (TMs) of comets were scored using CometScore software (TriTek, Sumerduck, VA, USA). Percent repair (% repair) was determined by monitoring the return to baseline TM levels ($TM_{no\ IR}/TM_{5h}$). Where no specific WT-LCL line is denoted, % repair values are normalized to multiple WT samples used across experimental replicates to avoid any unexpected idiosyncrasies specific to a particular WT line. Initial induction of DNA breaks (i.e., without time for DSB repair) was also measured by the NCA. LCLs were treated with 2 and 5 Gy and immediately placed on ice after IR to assess the level of induced damage. Samples were then re-suspended in 1% low-melting-point agarose and assayed as described above to determine the initial induced levels of DSBs, and the results are reported as the TM without IR (0 Gy) and post-2 and -5 Gy.

**IR-induced foci assay.** The $\gamma$-H2AX, 53BP1, RAD51, and BRCA1 (Millipore, Billerica, MA, USA; Santa Cruz Biotechnology, Santa Cruz Biotechnology, Santa Cruz, CA, USA and Novus Biologics, Littleton, CO, USA, respectively) IR-induced foci assay was performed as previously described.[43] For $\gamma$-H2AX and 53BP1 foci, cells were treated with 2 Gy and collected at 1, 4, 8, and 24 h. Cells were collected at 4, 8, and 24 h post-12 Gy for assessment of BRCA1 foci. RAD51 foci were assessed 8 h post-IR, as previously described.[43] Cells were plated on coverslips, fixed with 4% paraformaldehyde, permeabilized with 0.5% Triton-X 100 (Sigma-Aldrich), blocked in 10% FBS, and incubated with primary antibodies (1 : 300) for 1 h at room temperature. The coverslips were washed, blocked with 10% FBS, and incubated with a AlexaFluor-488 secondary antibody (1 : 400, Invitrogen) for 45 min at room temperature. Coverslips were washed a final time and mounted on slides using ProlongGold anti-fade reagent containing DAPI (Applied Biosystems, Grand Island, NY, USA). Foci were imaged using an Olympus fluorescent microscope equipped with an AxioVision camera and software. Cells were scored as positive if they contained four or more foci/nuclei and results are presented as percent positive cells (% Pos).

**Rezasurin assay.** Rezasurin is reduced to a fluorescent dye as mitochondria respire and has been used to monitor mitochondrial respiration in radiosensitive cells.[37,46] Cells were grown at low density, collected, and plated on a 96-well plate. Before plating, cells were resuspended in fresh media containing 3 mM of the rezasurin dye (Sigma-Aldrich). The plates were measured at 0, 1, 2, and 3 h post-plating to monitor the relative increase in fluorescence, which is indicative of respiration levels. Fluorescence levels were measured on a SpectraMax M5 plate reader (Molecular Devices, Sunnyvale, CA, USA).

**ROS assessment and Annexin V assay.** DCHF-DA was used to assess the presence of a broad array of cellular ROS levels, as previously described.[53] DHE preferentially detects superoxide moieties and was used to assess superoxide levels.[47] Cells were collected and re-suspended in 1 $\times$ PBS at 37 °C containing 50 $\mu$M DCHF-DA dye (Sigma) for 20 min or for 30 min in RPMI media containing 20 $\mu$M DHE dye (Life Technologies, Carlsbad, CA, USA). For the DCHF-DA dye, samples were treated with 10 Gy or sham treated and immediately placed on ice and analyzed within 8 min by FACS (FL-1). Samples incubated with DHE were also sham treated or irradiated with 10 Gy and analyzed by FACS (FL-2) within 8 min. Annexin V has been previously described to label apoptotic cells for rapid analysis by FACS.[54] The flow cytometry-based Annexin V Apoptosis kit was used per manufacturer's protocol (BD Biosciences, San Jose, CA, USA). Cells were collected 48 h post-10 Gy and re-suspended in 1 $\times$ binding buffer containing Annexin V and propidium iodide. Cells positive for Annexin V staining were scored as positive for apoptosis.

**Mitochondrial bioenergetics assay.** The mitochondrial bioenergetics assays were performed on the XF24 Extracellular Flux Analyzer (Seahorse Biosciences, Billerica, MA, USA) as previously described.[55,56] Briefly, $3 \times 10^5$ cells were re-suspended in RPMI media and added to each poly-D-lysine-coated well in an XF24 Analyzer 24-well plate. Four wells (i.e., four replicates) were used for each cell line and condition measured. The plate was then centrifuged for 1 min and incubated at 37 °C and 5% $CO_2$ for 30 min to allow suspension cells to attach to the plate before analysis. Measurements were carried out after addition of Oligo, FCCP, and rotenone/myxothiazol at concentrations of 0.75 $\mu$M for each compound to act as an ATP synthase inhibitor, respiratory chain uncoupler, and mitochondrial respiration inhibitors, respectively. A 2-min mix and 2-min wait period preceded measurement of the oxygen consumption rate during a 4-min measurement period for each cycle of the XF24 analyzer.

**Exome sequencing and variant calling.** At the time of initial sequencing, only one LCL was available, RS63-3. Exonic sequences from RS63-3 were captured using Agilent SureSelect v1 (Agilent, Santa Clara,

CA, USA) and submitted for 50 base pair, paired end sequencing on an Illumina HiSeq instrument (Illumina, San Diego, CA, USA). A total of 9 GB of sequence was obtained and aligned to the human reference genome (GRCh37). The median read depth was 78x; 91.68% of the exome was sequenced to a depth of 20x or greater. After alignment to the human reference genome, duplicate molecules arising during PCR were removed with the MarkDuplicates utility in Picard (version 1.60; Source Forge, http://picard.sourceforge.net). In the interest of improved insertion-deletion (INDEL) discovery, alignments supporting candidate INDELs were realigned with the GATK (version 1.4.9; Broad Institute, http://broadinstitute.org/gatk) IndelRealigner utility.[57] Both single-nucleotide and INDEL polymorphisms were identified with the GATK UnifiedGenotyper (version 1.4.9) using default settings and all variants were annotated and prioritized with GEMINI.[58]

**Statistics.** Unless otherwise noted, data are presented as the mean of three independent measurements ($n=3$) and error bars represent $\pm 1$ standard deviation. Statistical analysis was determined by the Student's *t*-test for two independent samples of equal variance and *P*-values of $P<0.05$ were considered significant.

## Conflict of Interest

The authors declare no conflict of interest.

**Acknowledgements**. We thank Dr. Laurent Vergnes for his technical assistance with the mitochondrial bioenergetics assay and Ms. Brandi Woo for her technical help profiling the DNA damage response in RS63-3 and -7. Flow cytometry was performed in the UCLA Jonsson Comprehensive Cancer Center (JCCC) and Center for AIDS Research Flow Cytometry Core Facility that is supported by National Institutes of Health awards CA-16042 and AI-28697, and by the JCCC, the UCLA AIDS Institute, and the David Geffen School of Medicine at UCLA.

1. Gatti RA. The inherited basis of human radiosensitivity. *Acta Oncol* 2001; **40**: 702–711.
2. Nahas SA, Gatti RA. DNA double strand break repair defects, primary immunodeficiency disorders, and 'radiosensitivity'. *Curr Opin Allergy Clin Immunol* 2009; **9**: 510–516.
3. Kurz EU, Lees-Miller SP. DNA damage-induced activation of ATM and ATM-dependent signaling pathways. *DNA Repair* 2004; **3**: 889–900.
4. Sun X, Becker-Catania SG, Chun HH, Hwang MJ, Huo Y, Wang Z *et al.* Early diagnosis of ataxia-telangiectasia using radiosensitivity testing. *J Pediatr* 2002; **140**: 724–731.
5. Pollard JM, Gatti RA. Clinical radiation sensitivity with DNA repair disorders: an overview. *Int J Radiat Oncol Biol Phys* 2009; **74**: 1323–1331.
6. Taylor AMR, Harnden DG, Arlett CF, Harcourt SA, Lehmann AR, Stevens S *et al.* Ataxia telangiectasia: a human mutation with abnormal radiation sensitivity. *Nature* 1975; **258**: 427–429.
7. Lee J-H, Paull TT. ATM activation by DNA double-strand breaks through the Mre11-Rad50-Nbs1 complex. *Science* 2005; **308**: 551–554.
8. Barbi G, Scheres JM, Schindler D, Taalman RD, Rodens K, Mehnert K *et al.* Chromosome instability and X-ray hypersensitivity in a microcephalic and growth-retarded child. *Am J Med Genet* 1991; **40**: 44–50.
9. Hiel JA, Weemaes CM, van Engelen BG, Smeets D, Ligtenberg M, van Der Burgt I *et al.* Nijmegen breakage syndrome in a Dutch patient not resulting from a defect in NBS1. *J Med Genet* 2001; **38**: E19.
10. Kobayashi J, Kato A, Ota Y, Ohba R, Komatsu K. Bisbenzamidine derivative, pentamidine represses DNA damage response through inhibition of histone H2A acetylation. *Mol Cancer* 2010; **9**: 34.
11. Waltes R, Kalb R, Gatei M, Kijas AW, Stumm M, Sobeck A *et al.* Human RAD50 dficiency in a Nijmegen breakage syndrome-like disorder. *Am J Hum Genet* 2009; **84**: 605–616.
12. Abraham RT. Cell cycle checkpoint signaling through the ATM and ATR kinases. *Genes Dev* 2001; **15**: 2177–2196.
13. Berkovich E, Monnat RJ, Kastan MB. Roles of ATM and NBS1 in chromatin structure modulation and DNA double-strand break repair. *Nat Cell Biol* 2007; **9**: 683–690.
14. Falck J, Coates J, Jackson SP. Conserved modes of recruitment of ATM, ATR and DNA-PKcs to sites of DNA damage. *Nature* 2005; **434**: 605–611.
15. Uziel T, Lerenthal Y, Moyal L, Andegeko Y, Mittelman L, Shiloh Y. Requirement of the MRN complex for ATM activation by DNA damage. *EMBO J* 2003; **22**: 5612–5621.
16. Paull TT, Rogakou EP, Yamazaki V, Kirchgessner CU, Gellert M, Bonner WM. A critical role for histone H2AX in recruitment of repair factors to nuclear foci after DNA damage. *Curr Biol* 2000; **10**: 886–895.
17. Doil C, Mailand N, Bekker-Jensen S, Menard P, Larsen DH, Pepperkok R *et al.* RNF168 binds and amplifies ubiquitin conjugates on damaged chromosomes to allow accumulation of repair proteins. *Cell* 2009; **136**: 435–446.
18. Devgan SS, Sanal O, Doil C, Nakamura K, Nahas SA, Pettijohn K *et al.* Homozygous deficiency of ubiquitin-ligase ring-finger protein RNF168 mimics the radiosensitivity syndrome of ataxia-telangiectasia. *Cell Death Differ* 2011; **18**: 1500–1506.
19. Stewart GS, Panier S, Townsend K, Al-Hakim AK, Kolas NK, Miller ES *et al.* The RIDDLE syndrome protein mediates a ubiquitin-dependent signaling cascade at sites of DNA damage. *Cell* 2009; **136**: 420–434.
20. Chapman JR, Sossick AJ, Boulton SJ, Jackson SP. BRCA1-associated exclusion of 53BP1 from DNA damage sites underlies temporal control of DNA repair. *J Cell Sci. 2012* **125**: 3529–3534.
21. Lottersberger F, Bothmer A, Robbiani DF, Nussenzweig MC, de Lange T. Role of 53BP1 oligomerization in regulating double-strand break repair. *Proc Natl Acad Sci USA* 2013; **110**: 2146–2151.
22. Aly A, Ganesan S. BRCA1, PARP, and 53BP1: conditional synthetic lethality and synthetic viability. *J Mol Cell Biol* 2011; **3**: 66–74.
23. Hu Y, Scully R, Sobhian B, Xie A, Shestakova E, Livingston DM. RAP80-directed tuning of BRCA1 homologous recombination function at ionizing radiation-induced nuclear foci. *Genes Dev* 2011; **25**: 685–700.
24. Martin NT, Nakamura K, Davies R, Nahas SA, Brown C, Tunuguntla R *et al.* ATM–dependent miR-335 targets CtIP and modulates the DNA damage response. *PLoS Genet* 2013; **9**: e1003505.
25. Cousineau I, Abaji C, Belmaaza A. BRCA1 regulates RAD51 function in response to DNA damage and suppresses spontaneous sister chromatid replication slippage: Implications for sister chromatid cohesion, genome stability, and carcinogenesis. *Cancer Res* 2005; **65**: 11384–11391.
26. Pellegrini L, Yu DS, Lo T, Anand S, Lee M, Blundell TL *et al.* Insights into DNA recombination from the structure of a RAD51-BRCA2 complex. *Nature* 2002; **420**: 287–293.
27. Caputo F, Vegliante R, Ghibelli L. Redox modulation of the DNA damage response. *Biochem Pharmacol* 2012; **84**: 1292–1306.
28. Hosoki A, Yonekura S, Zhao QL, Wei ZL, Takasaki I, Tabuchi Y *et al.* Mitochondria-targeted superoxide dismutase (SOD2) regulates radiation resistance and radiation stress response in HeLa cells. *J Radiat Res* 2012; **53**: 58–71.
29. Kaneyuki Y, Yoshino H, Kashiwakura I. Involvement of intracellular reactive oxygen species and mitochondria in the radiosensitivity of human hematopoietic stem cells. *J Radiat Res* 2012; **53**: 145–150.
30. Hopfner KP, Karcher A, Shin DS, Craig L, Arthur LM, Carney JP *et al.* Structural biology of Rad50 ATPase: ATP-driven conformational control in DNA double-strand break repair and the ABC-ATPase superfamily. *Cell* 2000; **101**: 789–800.
31. Cadet J, Ravanat J-L, TavernaPorro M, Menoni H, Angelov D. Oxidatively generated complex DNA damage: Tandem and clustered lesions. *Cancer Lett* 2012; **327**: 5–15.
32. Sedelnikova OA, Redon CE, Dickey JS, Nakamura AJ, Georgakilas AG, Bonner WM. Role of oxidatively induced DNA lesions in human pathogenesis. *Mutat Res* 2010; **704**: 152–159.
33. Porcedda P, Turinetto V, Lantelme E, Fontanella E, Chrzanowska K, Ragona R *et al.* Impaired elimination of DNA double-strand break-containing lymphocytes in ataxia telangiectasia and Nijmegen breakage syndrome. *DNA Repair* 2006; **5**: 904–913.
34. Kulkarni R, Marples B, Balasubramaniam M, Thomas RA, Tucker JD. Mitochondrial gene expression changes in normal and mitochondrial mutant cells after exposure to ionizing radiation. *Radiat Res* 2010; **173**: 635–644.
35. Kulkarni R, Reither A, Thomas RA, Tucker JD. Mitochondrial mutant cells are hypersensitive to ionizing radiation, phleomycin and mitomycin C. *Mutat Res* 2009; **663**: 46–51.
36. Kulkarni R, Thomas RA, Tucker JD. Expression of DNA repair and apoptosis genes in mitochondrial mutant and normal cells following exposure to ionizing radiation. *Environ Mol Mutagen* 2011; **52**: 229–237.
37. Nahas SA, Davies R, Fike F, Nakamura K, Du L, Kayali R *et al.* Comprehensive profiling of radiosensitive human cell lines with DNA damage response assays identifies the neutral comet assay as a potential surrogate for clonogenic survival. *Radiat Res* 2012; **177**: 176–186.
38. Crosby AH, Patel H, Chioza BA, Proukakis C, Gurtz K, Patton MA *et al.* Defective mitochondrial mRNA maturation is associated with spastic ataxia. *Am J Hum Genet* 2010; **87**: 655–660.
39. Adzhubei I, Jordan DM, Sunyaev SR. Predicting functional effect of human missense mutations using PolyPhen-2. *Curr Protoc Hum Genet* 2013; Chapter 7, Unit 7; 20.
40. Bai Y, Srivastava SK, Chang JH, Manley JL, Tong L. Structural basis for dimerization and activity of human PAPD1, a noncanonical poly(A) polymerase. *Mol Cell* 2011; **41**: 311–320.
41. Slomovic S, Schuster G. Stable PNPase RNAi silencing: its effect on the processing and adenylation of human mitochondrial RNA. *RNA* 2008; **14**: 310–323.
42. Kitagawa R, Bakkenist CJ, McKinnon PJ, Kastan MB. Phosphorylation of SMC1 is a critical downstream event in the ATM-NBS1-BRCA1 pathway. *Genes Dev* 2004; **18**: 1423–1438.
43. Martin NT, Nahas SA, Tunuguntla R, Fike F, Gatti RA. Assessing 'radiosensitivity' with kinetic profiles of gamma-H2AX, 53BP1 and BRCA1 foci. *Radiother Oncol* 2011; **101**: 35–38.

44. Yun MH, Hiom K. CtIP-BRCA1 modulates the choice of DNA double-strand-break repair pathway throughout the cell cycle. *Nature* 2009; **459**: 460–463.
45. Pagano G, Degan P, D'Ischia M, Kelly FJ, Nobili B, Pallardó FV *et al.* Oxidative stress as a multiple effector in Fanconi anaemia clinical phenotype. *Eur J Haematol* 2005; **75**: 93–100.
46. Ambrose M, Goldstine JV, Gatti RA. Intrinsic mitochondrial dysfunction in ATM-deficient lymphoblastoid cells. *Hum Mol Genet* 2007; **16**: 2154–2164.
47. Peshavariya HM, Dusting GJ, Selemidis S. Analysis of dihydroethidium fluorescence for the detection of intracellular and extracellular superoxide produced by NADPH oxidase. *Free Radic Res* 2007; **41**: 699–712.
48. Rochette L, Ghibu S, Richard C, Zeller M, Cottin Y, Vergely C. Direct and indirect antioxidant properties of $\alpha$-lipoic acid and therapeutic potential. *Mol Nutr Food Res* 2013; **57**: 114–125.
49. Reliene R, Pollard JM, Sobol Z, Trouiller B, Gatti RA, Schiestl RH. N-acetyl cysteine protects against ionizing radiation-induced DNA damage but not against cell killing in yeast and mammals. *Mutat Res* 2009; **665**: 37–43.
50. Zhou L, Jin J, Song G, Liu H, Liu M, Shi C *et al.* alpha-Lipoic acid ameliorates mitochondrial impairment and reverses apoptosis in FABP3-overexpressing embryonic cancer cells. *J Bioenerg Biomembr* 2013; **45**: 459–466.
51. Murphy MP. How mitochondria produce reactive oxygen species. *Biochem J* 2009; **417**: 1–13.
52. Kang MA, So EY, Simons AL, Spitz DR, Ouchi T. DNA damage induces reactive oxygen species generation through the H2AX-Nox1/Rac1 pathway. *Cell Death Dis* 2012; **3**: e249.
53. Hafer K, Iwamoto KS, Schiestl RH. Refinement of the dichlorofluorescein assay for flow cytometric measurement of reactive oxygen species in irradiated and bystander cell populations. *Radiat Res* 2008; **169**: 460–468.
54. Vermes In, Haanen C, Steffens-Nakken H, Reutellingsperger C. A novel assay for apoptosis flow cytometric detection of phosphatidylserine expression on early apoptotic cells using fluorescein labelled Annexin V. *J Immunol Methods* 1995; **184**: 39–51.
55. Wu M, Neilson A, Swift AL, Moran R, Tamagnine J, Parslow D *et al.* Multiparameter metabolic analysis reveals a close link between attenuated mitochondrial bioenergetic function and enhanced glycolysis dependency in human tumor cells. *Am J Physiol Cell Physiol* 2007; **292**: C125–C136.
56. Gerencser AA, Neilson A, Choi SW, Edman U, Yadava N, Oh RJ *et al.* Quantitative microplate-based respirometry with correction for oxygen diffusion. *Anal Chem* 2009; **81**: 6868–6878.
57. McKenna A, Hanna M, Banks E, Sivachenko A, Cibulskis K, Kernytsky A *et al.* The Genome Analysis Toolkit: a MapReduce framework for analyzing next-generation DNA sequencing data. *Genome Res* 2010; **20**: 1297–1303.
58. Paila U, Chapman BA, Kirchner R, Quinlan AR. GEMINI: integrative exploration of genetic variation and genome annotations. *PLoS Comput Biol* 2013; **9**: e1003153.

***Cell Death and Disease*** **is an open-access journal published by** ***Nature Publishing Group*****. This work is licensed under a Creative Commons Attribution-NonCommercial-ShareAlike 3.0 Unported License. To view a copy of this license, visit http://creativecommons.org/licenses/by-nc-sa/3.0/**

Supplementary Information accompanies this paper on Cell Death and Disease website (http://www.nature.com/cddis)